Biogeosciences Discuss., doi:10.5194/bg-2015-652, 2016
Manuscript under review for journal Biogeosciences
Published: 11 February 2016
© Author(s) 2016. CC-BY 3.0 License.

Biogeosciences Discussions
Open Access
EGU

The asynchronous response of carbon gain and water loss generate spatio-temporal pattern of WUE along elevation gradient in southwest China

Sun Xiangyang[1] Huang Mei[2] Wang Genxu[1]*

1. Institute of Mountain Hazards and Environment, Chinese Academy of Sciences, Chengdu Sichuan 610041
2. Institute of Geographic Sciences and Natural Resources Research, Chinese Academy of Sciences, Beijing 100101

Corresponding author: Wang Genxu, wanggx@imde.ac.cn, Institute of Mountain Hazards and Environment, Chinese Academy of Sciences, #.9, Block 4, Renminnanlu Road, Chengdu Sichuan 610041, +86-28-85233420

Biogeosciences Discuss., doi:10.5194/bg-2015-652, 2016
Manuscript under review for journal Biogeosciences
Published: 11 February 2016
© Author(s) 2016. CC-BY 3.0 License.

Abstract: The ratio of carbon gain to water loss, or water use efficiency (WUE), is a key characteristic of ecosystem function, and reflects the trade-off relationship between carbon gain and evapotranspiration (ET). The carbon and water cycles are very complex at the ecosystem scale, especially along altitudinal gradients. A stable carbon isotope method and the AVIM2 model were used to study the temporal and altitudinal patterns of carbon gain, water loss and ecosystem WUE in dark coniferous forests (*Abies fabri*) in subalpine, Southwest China. WUE was defined using different components of carbon gain and water loss. The temporal and altitudinal variations of WUE were found. WUE in the vegetative season was larger than in the dormant season. Climatic conditions such as monthly precipitation, air temperature, vapor pressure deficit (VPD) and net radiation contributed to the monthly variation in ecosystem WUE. Both the carbon gain and water loss decreased as the altitude increased, and the carbon gain exhibited a moderately decreasing rate compared with that of the water loss along the altitude gradient. WUE exhibited an increasing trend along the elevation gradient, but discrepancies appeared when different definitions of WUE were used. Variations in WUE indicated different coupling relationships between the carbon gain and water loss on different temporal and altitudinal scales. The asynchronous response of the carbon gain and water loss to climatic and physiological variables determined the temporal and altitudinal patterns of ecosystem WUE.

Keywords: Water use efficiency, dark coniferous forest, temporal, elevation, southwestern China

Biogeosciences Discuss., doi:10.5194/bg-2015-652, 2016
Manuscript under review for journal Biogeosciences
Published: 11 February 2016
© Author(s) 2016. CC-BY 3.0 License.

1. Introduction

The carbon and water cycles of terrestrial ecosystems are key ecological processes that are tightly coupled via the ecosystem water use efficiency (WUE, the mass ratio of CO_2 assimilated during photosynthesis to evaporated or transpired H_2O) (Yu GR et al., 2008; Beer et al., 2009; Keenan et al., 2013). The carbon and water cycles are very complex on the ecosystem scale, especially along altitudinal gradients, these cycles are influenced by variations in climate (Goulden et al., 2012) and plant physiology (Hultine and Maeshell, 2000; Li CY et al., 2009). The WUE is an important indicator of the coupled relationship between the carbon cycle and the water cycle (Alice et al., 2011). The variation of the $\delta^{13}C$ in bulk leaf tissue has been described in southwestern China (Luo TX et al., 2005; Li CY et al., 2009; Li JZ et al., 2009), but the altitudinal and seasonal patterns of carbon gain and water loss are poorly understood.

Knowledge of WUE along altitude gradients is critical to understand the potential responses of trees to climate change. Farquhar et al. (1982, 1989) found that the stable carbon isotope composition of leaf tissue was related to c_i/c_a and can therefore be used to calculate the intrinsic water use efficiency. Over the past several decades, $\delta^{13}C$ has been widely used as an indicator of intrinsic WUE on different scales such as the leaf, plant and ecosystem scales (Bonal et al., 2000; Lauteri et al., 2004; Sauer et al., 2004; Ponton et al., 2006). Most studies have demonstrated that altitude has a positive effect on $\delta^{13}C$ in the subalpine zone (Hultine and Marshall, 2000; Li et al., 2004; Li CY et al., 2009). Bert et al. (1997) found that WUE increased by 30% from the 1930s to the 1980s. In order to fully understand WUE along altitude, we still need to study different

Biogeosciences Discuss., doi:10.5194/bg-2015-652, 2016
Manuscript under review for journal Biogeosciences
Published: 11 February 2016
© Author(s) 2016. CC-BY 3.0 License.

response of carbon gain and water loss to environmental variables.

The seasonal patterns of WUE and its components reveal how mechanisms that lead to long-term and altitudinal WUE vary by plant functional type. WUE are controlled by environmental factors, such as the soil water content, atmospheric CO_2 concentration, air temperature, vapor pressure deficit and solar radiation, and physiological factors such as canopy conductance and nutrient content (Hultine and Maeshell, 2000; Li Chunyang et al., 2009; Goulden et al., 2012). Evapotranspiration (ET) accounts for up to 95% of the water loss from an ecosystem (Huxman et al., 2005). Recent studies have paid more attention to the seasonal variation of WUE with changes in the global climate (Yu GR et al., 2009; Keenan et al., 2013; Li SE et al., 2015). However, the responses of the carbon gain and water loss to climatic variables and canopy conductance depend on the forest types and even seasons. The temporal and altitudinal variations in ecosystem WUE are largely unexplained (Reichstein et al., 2014). Further research is needed to reveal the main influences and the response relationships among the carbon gain, water loss and environmental factors for different forest types.

Moreover, both the carbon gain and water loss consist of distinct components. For ecosystems, WUE is expressed as the ratio of net or gross ecosystem production to water loss (Law et al., 2002). However, the definitions and meanings of WUE expressed by different components of carbon gain and water loss were different (Yu GR et al., 2009; Hu ZM et al., 2010), or were only weakly correlated (Ito and Inatomi, 2012). Therefore, different definitions of WUE cannot be compared directly.

Biogeosciences Discuss., doi:10.5194/bg-2015-652, 2016
Manuscript under review for journal Biogeosciences
Published: 11 February 2016
© Author(s) 2016. CC-BY 3.0 License.

Abies is the dominant species in coniferous forests of the Northern Hemisphere (Wang et al., 2014). Most *Abies* are distributed over a broad vertical range in mountainous regions. *Abies* also form typical subalpine dark coniferous forests in southwestern China (Lv et al., 2009). The mountainous area in southwestern China is the source region of 6 main rivers and the second largest forest area in China (Sun HL, 2005; Wang GX et al., 2011). The subalpine coniferous forest is highly sensitive to climate change (Gao and Wang, 2007). *Abies* play an important role in the trade-off relationship between carbon storage and water resources. The temporal and altitudinal pattern of WUE in subalpine forests in southwestern China is still not characterized despite obvious practical importance. To address these questions, both model and stable isotope methods are adopted to simulate and elucidate the carbon gain, water loss and their components. The AVIM2 (Atmospheric-vegetation interaction model) was performed to simulate GPP, NPP, ET and its three components. The aim of this study is to 1) analyze the temporal and altitudinal pattern of the ecosystem WUE using a different definition for *Abies fabri*, 2) demonstrate why WUE of *Abies fabri* increased or decreased with altitude in the subalpine mountains.

2. Materials and methods

2.1. Study area

The study was conducted at Gongga Mountain (29°20′–30°20′ N, 101°30′–102°15′ E), which is located in the transitional area between the eastern monsoon subtropics of China and the frigid region of the Tibetan Plateau. It is the summit of Hengduan Mountain. The climate is dominated by the southeastern Pacific monsoon. The annual

Biogeosciences Discuss., doi:10.5194/bg-2015-652, 2016
Manuscript under review for journal Biogeosciences
Published: 11 February 2016
© Author(s) 2016. CC-BY 3.0 License.

111 mean air temperature in this region is 3.9 °C at an altitude of 3000 m, and the annual
112 rainfall is 1940 mm, with most rainfall events occurring between May and October,
113 which account for 79.7% of the annual rainfall. The relative humidity during the wet
114 season is 91%. The annual mean air temperature decreased at a rate of 0.6 °C per 100
115 m along the altitudinal gradient.

116 The wide altitude range (1100–7556 m) results in a diverse range of vegetation
117 zones, with forest types varying from subtropical to cold alpine vegetation. *A. fabri*,
118 which is a part of the dark coniferous forest, is the dominant tree species in study area
119 on the eastern slope of the Gongga Mountain from 2800 to 3700 m a.s.l (the alpine
120 treeline). The dark coniferous forest is the zonal vegetation of the cold temperate zone
121 and the widespread subalpine forest type in southwestern China and the northern
122 hemisphere. The soil has developed from granite and is classified as a mountain gray-
123 brown soil, which has a high sand content and strong permeability (He YR et al., 2005).

124 **2.2. AVIM2 model**

125 The GPP, NPP and ET were simulated using the Atmospheric-Vegetation
126 Interaction Model (AVIM2) that was developed for simulating seasonal and inter-
127 annual variations in biophysical and biogeochemical processes at the land surface. The
128 AVIM2 includes a physical process module (PHY), a physiological plant growth
129 module (PLT) and a soil carbon and nitrogen dynamics module (SOM).

130 2.2.1 Physical process module

131 PHY is a typical soil vegetation atmosphere transfer scheme (SVAT), which is
132 based on the work of Ji and Hu (1989), while for the new version of AVIM, snow

Biogeosciences Discuss., doi:10.5194/bg-2015-652, 2016
Manuscript under review for journal Biogeosciences
Published: 11 February 2016
© Author(s) 2016. CC-BY 3.0 License.

accumulation and snowmelt processes are added (Lu and Ji, 2006). The physical processes of PHY include the radiation transfer, the sensible and latent heat fluxes between the air, canopy and soil, the interception of rainfall and drainage, runoff and infiltration, transpiration from the canopy and evaporation from the surface, and snow accumulation and snowmelt processes. The components of ET consisted of canopy interception (Eint), transpiration (Et) from the canopy, evaporation from the soil (Es) and evaporation from snow cover. The other details of these processes are given by Ji and Hu (1989), Ji (1995) and Lu and Ji (2006).

2.2.2 Physiological plant growth module

The vegetation is separated into three components: the foliage, the fine roots and the remaining parts. Detailed descriptions of this process can be found in Ji et al (2005), Lu and Ji (2006) and Huang et al. (2007). When atmospheric CO_2 enters through the stomata, dry matter is produced via photosynthesis. The gross primary production (GPP) is calculated based on the Farquhar model, which is based on the biochemistry of photosynthesis (Farquhar et al., 1980):

$$\mathrm{GPP} = \min(w_c, w_j) \quad (1)$$

where w_c is the Rubisco-limited carboxylation rate, and w_j is the carboxylation rate limited by the rate of RuBP regeneration in the Calvin cycle. The carboxylation rate is a function of the environment temperature, leaf nitrogen concentration and leaf water potential.

The loss of dry matter is due to the respiration of the plant (R_t), which includes maintenance (R_m) and growth (R_g) components (Kozlowski, 1992).

Biogeosciences Discuss., doi:10.5194/bg-2015-652, 2016
Manuscript under review for journal Biogeosciences
Published: 11 February 2016
© Author(s) 2016. CC-BY 3.0 License.

$$R_t = R_m + R_g = \mathrm{a} \cdot \mathrm{BM} + \mathrm{b}\frac{dBM}{dt} \quad (2)$$

where *BM* is the total living biomass, which is the sum of the foliage, fine roots and remaining parts, and t is the time step.

The residue of gross photosynthesis minus total respiration, which is named net primary productivity (NPP), is allocated to plant organs.

$$\mathrm{NPP} = A_c - R_m - R_g \quad (3)$$

Then, the changing rates of biomass for leaves, stems and root are as follows:

$$(1+\mathrm{b})\frac{dM_f}{dt} = \alpha_f(A_c - R_m) - \mu_f M_f \quad (4)$$

$$(1+\mathrm{b})\frac{dM_r}{dt} = \alpha_r(A_c - R_m) - \mu_r M_r \quad (5)$$

$$(1+\mathrm{b})\frac{dM_s}{dt} = \alpha_s(A_c - R_m) - \mu_s M_s \quad (6)$$

where M_f, M_s, M_r are the biomass of the leaves, stems and roots, respectively. The subscripts f, s and r denote the variables for leaves, stems and roots, respectively. α_f, α_r and α_s are the allocating coefficients of assimilated matter, with $\alpha_f + \alpha_r + \alpha_s = 1$. μ_f, μ_r and μ_s are the rates of litterfall.

2.2.3 Soil carbon and nitrogen dynamics module

The SOM simulates the transformation and decomposition of soil organic carbon and nitrogen mineralization. It was developed on the basis of soil carbon and nitrogen dynamics modules of CENTURY (Parton et al., 1987) and CEVSA (Cao and Woodward, 1998). The soil organic matter was divided into eight pools, i.e. surface structural and metabolic litter, structural and metabolic root litter, surface microbes and soil microbe, slow and passive carbon. The split of plant residue into metabolic (F_M) and structural components (F_S) are determined as a function of the lignin/nitrogen ratio (L/N), as

Biogeosciences Discuss., doi:10.5194/bg-2015-652, 2016
Manuscript under review for journal Biogeosciences
Published: 11 February 2016
© Author(s) 2016. CC-BY 3.0 License.

177 shown by the following equation (Parton et al., 1987):

178 $$F_M = 0.85 - 0.018\,L/N \quad (7)$$

179 $$F_S = 1 - F_M \quad (8)$$

180 All carbon transformations between these eight pools and be decomposed of each
181 pool is expressed as followed:

182 $$\frac{dQ_i}{dt} = K_i f(T) f(W) Q_i + d_{ij} Q_i + F \quad (9)$$

183 Where Q_i is the carbon density of each pool, K_i is maximum decomposition rate,
184 $f(T)$, $f(W)$ is the effect of soil temperature and moisture on decomposition rate, d_{ij} is the
185 transformational rate between pools and F is the input of litter carbon.

186 The sum of gaseous carbon loss from various soil carbon pools caused by
187 microbial decomposition is heterotrophic respiration (HR):

188 $$\mathrm{HR} = \sum_i Q_i K_i (1 - \varepsilon) \quad (10)$$

189 Where ε is the assimilation efficiency (Parton et al., 1993). HR minus NPP is the
190 net ecosystem exchange (NEE), that is, the net carbon flux between ecosystem and
191 atmosphere.

192 **2.3. Stable carbon isotope**

193 During the growing season (from May to October 2012), foliage samples of *Abies*
194 *fabri* were collected between 2,800 m and 3,700 m at 100-m intervals along the
195 altitudinal gradient of Mt. Gongga. At each altitude, we set out 50×100-m sampling
196 quadrats, where four to five trees were selected for sampling. A total of 20-30 trees
197 were selected at each altitude. Foliage samples were dried in a forced-draft oven at
198 65 °C for 48 h and then ground into a fine powder and stored at 4 °C until analysis.

Biogeosciences Discuss., doi:10.5194/bg-2015-652, 2016
Manuscript under review for journal Biogeosciences
Published: 11 February 2016
© Author(s) 2016. CC-BY 3.0 License.

199 The carbon isotopes were measured using an elemental analyzer (Flash EA1112
200 HT) interfaced to an isotope ratio mass spectrometer (MAT253, Thermo Fisher
201 Scientific, Inc., USA) at the Chinese Academy of Forestry. Subsamples of the foliage
202 biomass were analyzed for $^{13}C/^{12}C$ carbon isotope composition (expressed using delta-
203 notation, $\delta^{13}C_{PDB}$,‰) of CO_2 gas that was generated from the combustion of the dried
204 foliage tissue in an elemental analyzer. The precision of the $\delta^{13}C$ measurements was
205 0.1% based on the standard deviation of repeated analyses. The ratio of stable carbon
206 isotope (perl mil, ‰) is expressed as follows (Farquhar et al., 1989):

207 $$\delta^{13}C_p = (R_{sample}/R_{std} - 1) \times 1000 \quad (11)$$

208 Where R_{sample} and R_{std} are the ratio of the heavy to light isotope in the sample and the
209 international Vienna Pee Dee Belemnite carbon standard material, respectively.

210 Farquhar et al. (1982) showed that there was a relationship between the stable
211 carbon isotope composition of leaf tissue and c_i/c_a.

212 $$\delta^{13}C_p = \delta^{13}C_a - a - (b - a)\frac{c_i}{c_a} \quad (12)$$

213 where a is the isotopic fractionation during photosynthetic gas exchange caused by the
214 slower diffusion of $^{13}CO_2$ in air (4‰), b is the net fractionation associated with RuBP
215 carboxylase activity (27‰), and c_i and c_a are the atmospheric and intercellular CO_2
216 concentrations, respectively.

217 WUE of the ecosystem from $\delta^{13}C_p$ measurements can be expressed by the
218 following equation:

219 $$\mathrm{WUE} = \frac{A}{E} = \frac{c_a - c_a(\delta^{13}C_p - \delta^{13}C_a - a)/(b-a)}{1.6\Delta W} \quad (13)$$

220 where ΔW is the difference in the water vapor concentration between the intercellular

Biogeosciences Discuss., doi:10.5194/bg-2015-652, 2016
Manuscript under review for journal Biogeosciences
Published: 11 February 2016
© Author(s) 2016. CC-BY 3.0 License.

and ambient air, and the value 1.6 is the ratio of the stomatal conductance of water vapor to that of CO_2. In this study, ΔW represents the saturated vapor pressure deficit.

2.4 Eddy covariance measurements

Eddy covariance measurements of the carbon flux, latent and sensible heats were collected in 2009 at 30-minute intervals. An open-path eddy covariance system was installed 30 m above the ground in an *Abies fabri* experimental plot at an altitude of 3000 m. The system consisted of an open-path infrared gas analyzer (Li-7500; Licor Inc., Lincoln, NB, USA) and a three-dimensional sonic anemometer (CSAT3; Campbell Scientific Inc., Logan, UT, USA). A data logger (CR3000; Campbell Scientific Inc., Logan, UT, USA) recorded the eddy covariance signals at 10 Hz for archiving and online computation.

A three-angle coordinate rotation approach was used to align the coordinates (Wilczak et al., 2001). The WPL method was used to adjust density changes resulting from fluctuations in heat and water vapor (Webb et al., 1980). The friction velocity threshold was empirically set as 0.2 m s^{-1} to filter nighttime fluxes. Spurious data were removed from the dataset if the instrument performance was abnormal or rainfall events occurred. The missing data accounted for approximately 35% of the total data. To compare the simulated carbon and water fluxes, the missing or rejected data were not interpolated. The energy balance closure was evaluated using linear regression coefficients between the 30-minute estimates of dependent flux variables (LE+H) against the independently derived available energy (Rn-G-S) (Wilson et al., 2002). The closure of the energy balance was acceptable, the slope of LE+H vs. Rn-G-S was 0.71

Biogeosciences Discuss., doi:10.5194/bg-2015-652, 2016
Manuscript under review for journal Biogeosciences
Published: 11 February 2016
© Author(s) 2016. CC-BY 3.0 License.

(Lin et al., 2011).

2.4. Definition of WUE

The amount of carbon gained per unit of water loss is named WUE. WUE has different definitions depending on the temporal and spatial scales of the processes (Steduto and Albrizio, 2005), while the different definitions of WUE refer to different ecological processes and therefore, different influencing factors. In this study, WUE was calculated using the following equations:

$$\mathrm{WUE} = GPP/ET \quad (14)$$

$$\mathrm{WUE} = NPP/ET \quad (15)$$

WUE calculated using Eq. 14 and Eq. 15 are controlled by both the physiological process of transpiration and the physical process of evaporation from the soil surface and the canopy.

$$\mathrm{WUE} = GPP/Et \quad (16)$$

$$\mathrm{WUE} = \mathrm{NPP}/\mathrm{Et} \quad (17)$$

WUE calculated using Eq. 16 and Eq. 17 reflect the water use ability of the plant community.

WUE calculated using Eq. 14 and Eq. 15 are on the ecosystem scale, while those calculated using Eq. 16 and Eq. 17 are on the plant scale. The difference is the sum of the canopy interception and soil evaporation.

2.5. Data and the validation of the model

The hourly meteorological data (January to December, 2012) used as model inputs, include the hourly mean air temperature, precipitation, relative humidity, wind velocity

Biogeosciences Discuss., doi:10.5194/bg-2015-652, 2016
Manuscript under review for journal Biogeosciences
Published: 11 February 2016
© Author(s) 2016. CC-BY 3.0 License.

and radiation, and were collected at altitudes of 2200 m, 3000 m, 3500 m and 4200 m by an auto meteorological observation system (AMOS) on Mt. Gongga. According to the observations of the four AMOSs, the wind velocity, relative humidity and total radiation rarely varied. Because our study was carried out in the Hailuogou valley on the same aspect, linear interpolation was used to interpolate the air temperature and precipitation along the elevation gradient every 100 m. Linear interpolation was used to derive the temperature and precipitation along the altitudinal gradient.

The model validation tests the degree of agreement between the simulated and measured values. The AVIM2 has been validated by many vegetation types in China, such as forest, crops, steppe and desert grassland (Lu and Ji, 2006; Huang et al., 2007; Ji et al., 2008). The modeled WUE, which is defined as GPP/Et, was validated by comparing the simulated value to that derived from $\delta^{13}C$. The results demonstrated that WUE (GPP/Et) simulated by the AVIM2 was generally in agreement in terms of temporal and altitudinal variations with the measured WUE (Fig. 1a, b). The analysis of R-squared (R^2) and *p* value indicated that the simulated value had good accuracy. The simulated NEE was also compared with that observed by eddy covariance, and the results showed that the AVIM2 can capture the variance of NEE (Fig. 2).

The simulated ET was also validated with the value observed by eddy covariance. The AVIM2 can simulate the daily variation of the ET in the vegetative season or in the dormant season (Fig. 3). The components of the ET were also validated with the observed results. The Eint, T and Es were observed from April to October in 2009 (Lin et al., 2011; Sun et al., 2013). The simulated canopy interception was 402.8 mm,

Biogeosciences Discuss., doi:10.5194/bg-2015-652, 2016
Manuscript under review for journal Biogeosciences
Published: 11 February 2016
© Author(s) 2016. CC-BY 3.0 License.

compared to 460.7 mm in observations (Sun et al., 2013). The simulated transpiration was 139.2 mm, which is almost the same as the observed value of 139.8 mm (Lin et al., 2011). The simulated evaporation from the ground was 56.3 mm, which is higher than the observed value of 44.2 mm (Lin et al., 2011). In conclusion, the AVIM2 was a convincing method for the simulation of the carbon gain and water loss on Gongga Mountain. Moreover, based on WUE derived from the $\delta^{13}C$, the ET, GPP and NPP simulated using the AVIM2 are also reliable.

2.6. Data analysis

A one-way ANOVA with Fisher's LSD test was performed to test the difference in the GPP, NPP, ET and WUE of different months. The relationships between the ET, Et, GPP and climatic variables were fitted with linear or non-linear equations using SigmaPlot 12.3. All analyses were conducted with SPSS 13.0. Statistically significant differences were set with $p < 0.05$.

3. Results

3.1. Seasonal variations of meteorological conditions

To reveal the relationship between WUE and climatic factors, the variation patterns of the monthly precipitation, air temperature, vapor pressure deficit (VPD) and net radiation (Rn) were investigated. The annual precipitation was 1896, 1606, 2022 and 1469 mm from 2008 to 2011 at an altitude of 3000 m (Fig. 4a). The annual mean air temperature was 4.7, 5.3, 5.4 and 4.6 °C, and the highest monthly mean air temperature occurred in July, while the coldest monthly mean air temperature was in December, January or February (Fig. 4b). Compared with the air temperature, the VPD

Biogeosciences Discuss., doi:10.5194/bg-2015-652, 2016
Manuscript under review for journal Biogeosciences
Published: 11 February 2016
© Author(s) 2016. CC-BY 3.0 License.

had a similar trend (Fig. 4c). In contrast to the air temperature, the maximum value of the monthly net radiation was not in July, possibly due to the large amount of rainfall and cloudy weather that contributed to the variation in this seasonal trend (Fig. 4d). Therefore, the carbon gain and the water loss were promoted or inhibited by these environmental conditions.

3.2. Seasonal and altitudinal variations of GPP and NPP

The monthly variations in GPP and NPP at an altitude of 3000 m from 2008 to 2011 were simulated using the AVIM2. Over the 4 years, both the GPP and NPP showed obvious seasonal variations. The peak values of GPP and NPP occurred in July, while the smallest values occurred in January or February (Fig. 5). The annual GPP and NPP were 5.8, 5.8, 6.0 and 6.2 $gCm^{-2}d^{-1}$ from 2008 to 2011. The mean monthly variations of GPP and NPP for *Abies fabri* at an elevation of 3000 m were also modeled using the AVIM2. During the period of dormancy (from November to April of the next year), the GPP and NPP were lower compared with the vegetative season, but plant photosynthesis and respiration continued even in the coldest month (air temperature < -5 °C). The annual GPP and NPP were 21143.7 and 12355.3 $kgC\ ha^{-1}\ a^{-1}$, respectively, at an altitude of 3000 m.

Both the GPP and NPP decreased as the altitude increased. The decreases were -0.09 and -0.03 $g\ m^{-2}\ s^{-1}$/100 m for the GPP and NPP, respectively. Both the GPP and NPP showed peak values at 3000 m (Fig. 6). The temperature decreased as the altitude increased, while the precipitation increased from an altitude of 2800 m to an altitude of 3500 m, before decreasing as the altitude increased further.

Biogeosciences Discuss., doi:10.5194/bg-2015-652, 2016
Manuscript under review for journal Biogeosciences
Published: 11 February 2016
© Author(s) 2016. CC-BY 3.0 License.

3.3. Seasonal and altitudinal variations of ET and its components

ET consists of canopy interception, transpiration and evaporation from the ground. The mean annual amounts of Eint, Et and Es at an altitude of 3000 m were 367.1, 247.7 and 91.5 mm, respectively. The ratio of annual Eint to ET was 51.3%. The ratio of Et increased from only 18.7% in January to a maximum of 43.5% in June. In contrast to the GPP and NPP, neither the Et nor the ET peaked in July (Fig. 7). The annual ET was 628, 640, 587 and 706 mm from 2008 to 2011. The annual Et was 187, 200, 195 and 248 mm from 2008 to 2011.

The ET decreased as the altitude increased (Fig. 8). The annual amount of Et decreased sharply. The ratio of Et to ET decreased from 48.9% at an altitude of 2800 m to 26.3% at an altitude of 3700 m. However, Eint had the inverse trend. More water was lost through Eint in the altitude range from 2800 m to 3700 m.

3.4. Seasonal and altitudinal variations of WUE

WUEs with different definitions all had a similar seasonal variation pattern: they were larger during the vegetative season and smaller after the vegetative season (Fig. 9). This pattern suggests that GPP/Et, GPP/Etotal, NPP/Et and NPP/Etotal were affected by meteorological conditions in different ways. However, the maximum values of GPP/Et and NPP/Et occurred in different months, which indicated that WUEs with different definitions were different from each other.

GPP/Et and NPP/Et increased significantly as the altitude increased (Fig. 10a), whereas the GPP/ET and NPP/ET increased from an altitude of 2800 to 3500 m and then slightly decreased from an altitude of 3600 to 3700 m (Fig. 10b). There exists a

Biogeosciences Discuss., doi:10.5194/bg-2015-652, 2016
Manuscript under review for journal Biogeosciences
Published: 11 February 2016
© Author(s) 2016. CC-BY 3.0 License.

353 yielding point at an altitude of 3000 m, and the GPP/ET and NPP/ET increased rapidly
354 under the altitude of 3000 m.

355 **4. Discussion**

356 **4.1 The definition of water use efficiency**

357 The different definitions of WUE in this study address the different characteristics
358 of the effects of ecosystem respiration and evaporation (canopy interception and
359 evaporation from ground) on the temporal and spatial patterns of ecosystem WUE.
360 Meanwhile, the WUE definitions were different for different levels of study. WUE is
361 usually defined as net or gross CO_2 assimilation at the cost of water loss via
362 transpiration at the canopy level. However, WUE is often defined as plant CO_2
363 assimilation at the cost of total water loss by ET at stand level. This discrepancy makes
364 it very difficult to compare WUEs of the same species derived from different water loss
365 and carbon gain components. The difference between GPP/Et and NPP/Et or between
366 GPP/ET and NPP/ET resulted from ecosystem respiration, which is sensitive to
367 temperature and soil moisture, whereas the difference between GPP/Et and GPP/ET or
368 between NPP/Et and NPP/ET is mainly determined by the ratio of Et/ET. The
369 transpiration and evaporation from the canopy and the soil were mainly controlled by
370 biological and environmental factors.

371 Forest ecosystems usually have high WUEs compared with grassland and cropland
372 ecosystems. Ponton et al. (2006) found that the value of GPP/ET were 1.7±0.5, 3.6±
373 1.5 and 5.4±1.6 mgC/gH_2O in grasslands, aspen and Douglasfir forests, respectively.
374 WUE expressed by GPP/ET was 2.5~3.1 mgC/gH_2O for *Abies fabri* along the

Biogeosciences Discuss., doi:10.5194/bg-2015-652, 2016
Manuscript under review for journal Biogeosciences
Published: 11 February 2016
© Author(s) 2016. CC-BY 3.0 License.

375 altitudinal gradient from 2800 m to 3700 m on Mt. Gongga. Compared with the results
376 reported in the literature, the values of GPP/ET in this research were in the normal range
377 (Law et al., 2002; Ponton et al., 2006; Yu GR et al., 2008; Beer et al., 2009).

378 The annual values of GPP/T, GPP/ET, NPP/T and NPP/ET were 7.1, 2.9, 4.2 and
379 1.8 mgC/gH_2O for *Abies fabri* at 3000 m on Mt. Gongga. Not only were the spatial and
380 temporal variations in WUE with different definitions different, but there was a large
381 amount of variation in the WUE value depending on the different definitions. Ito and
382 Inatomi (2012) also found that the values of GPP/T and NPP/ET were 8.0 and 0.92
383 mgC/gH_2O on the global scale. Meanwhile, GPP/T and NPP/ET were only weakly
384 correlated on the spatial scale (Ito and Inatomi, 2012).

385 **4.2 Seasonal patterns of water use efficiency**

386 There was a significant correlation between the carbon gain and water loss (Fig.
387 13), while the R^2 between the GPP, NPP and Et was larger than that of the GPP, NPP
388 and ET. Canopy interception was responsible for 51.3% of the total ET at 3000 m, and
389 the contribution was even higher as the altitude increased. Therefore, this non-stomatal
390 evaporation process reduced the strength of the correlation between the carbon gain and
391 water loss through the stomata. The carbon gain increased sharply as the water loss
392 increased when the monthly Et was less than 10 mm or the ET was less than 20 mm.
393 The patterns of the variations in carbon gain and water loss were relatively constant
394 throughout the vegetative season. The variations in WUE among different seasons, as
395 reported in the literature (Yu GR et al., 2007), indicated that the coupled relationship
396 between the carbon gain and water loss was influenced by changing climatic conditions.

Biogeosciences Discuss., doi:10.5194/bg-2015-652, 2016
Manuscript under review for journal Biogeosciences
Published: 11 February 2016
© Author(s) 2016. CC-BY 3.0 License.

397 The response of the carbon gain and water loss to climatic variables was different
398 in various forest ecosystems (Keenan et al., 2013; Medlyn and De Kauwe, 2013).
399 Understanding the effects of climatic variables on forest ecosystem productivity, WUE
400 is useful for the prediction of changes in the carbon gain and water loss due to climate
401 change (Law et al., 2002). In this study, the responsive characteristics of GPP, Et and
402 ET to monthly precipitation, temperature, VPD and net radiation (Rn) were analyzed at
403 an altitude of 3000 m.

404 The ET, Et and GPP responded to climatic variables differently. The relationships
405 between ET, Et, GPP and monthly precipitation and VPD were fitted with quadratic
406 functions (Fig. 14a, c). However, there were different relationships between ET, Et,
407 GPP, temperature and Rn (Fig. 14b, d). Temperature vs GPP, Rn vs ET and Rn vs T
408 were all fitted with linear functions. ET and Et decreased when $P > 180$ mm, while GPP
409 decreased when the monthly average Rn > 1700 MJ $m^{-2}d^{-1}$. The asynchronous
410 responses of ET, Et and GPP to changing climatic variables determined the relationship
411 between the carbon gain and water loss. Therefore, WUE with different definitions
412 varied during the month. The increasing rate of the ET and Et were much larger than
413 those of the GPP and NPP in the vegetative season. Although ET, Et and GPP were
414 fitted using the same mathematical form for monthly precipitation and VPD, the extent
415 to which these variations were due to climatic factors was different.

416 **4.3 Elevation gradients of water use efficiency**

417 An elevation gradient is not a phenomenological driving variable. However, it is
418 the combination of multiple factors, such as precipitation, temperature, nutrients and

Biogeosciences Discuss., doi:10.5194/bg-2015-652, 2016
Manuscript under review for journal Biogeosciences
Published: 11 February 2016
© Author(s) 2016. CC-BY 3.0 License.

419 plant physiology. The variation in precipitation had no significant influence on WUE
420 of *Abies fabri* along an altitudinal gradient in the Gongga Mountains (Fig. 11a), which
421 agreed with previous results (Li CY et al., 2009, Luo et al., 2011). A study in the
422 Hawaiian Metrosideros found that the $\delta^{13}C$ value of bulk leaf tissue increased as the
423 altitude increased in the eastern humid region, while the same trend did not exist in the
424 western arid region (Vitousek et al., 1990). The annual rainfall was more than 1600 mm
425 between 2800 m and 3700 m on the subalpine Gongga Mountain. Van de Water et al.
426 (2002) found that water was not the main influencing factor in the wet area. Therefore,
427 we concluded that the variation in the WUE along the altitudinal gradient was mainly
428 determined by other factors.

429 There was a significant negative relationship between the air temperature and
430 WUE derived from the $\delta^{13}C$ of bulk leaf tissue (Fig. 11b), which also indicated that the
431 intrinsic WUE increased as the air temperature decreased along the altitudinal gradient.
432 The curves of GPP and Et against temperature were different (Fig. 11b). Temperature
433 is an important climatic variable in mountainous terrain. The thicknesses and
434 hardnesses of leaves change to adapt to low temperature environments, while the
435 diffusion resistance to CO_2 also increases (Taylor and Sexton., 1972). As the diffusivity
436 decreased under low air temperature and soil temperature conditions, the stomatal
437 conductance also decreased (Panek and Warning, 1995). The transpiration was
438 restricted because the water potential of leaves increased when the air temperature and
439 soil temperature were low (Cochard et al., 2000). Therefore, the $\delta^{13}C$ of bulk leaf tissue
440 increased. Meanwhile, the GPP/Et and NPP/Et increased along the altitudinal gradient.

Biogeosciences Discuss., doi:10.5194/bg-2015-652, 2016
Manuscript under review for journal Biogeosciences
Published: 11 February 2016
© Author(s) 2016. CC-BY 3.0 License.

441 The $\delta^{13}C$ of bulk leaf tissue increased as the leaf nitrogen content increased
442 (R^2=0.9368, p<0.01) and decreased as the specific leaf area increased (R^2=0.9426,
443 p<0.01) (Fig. 12a, b). Hultien et al. (2000) found that a negative relationship existed
444 between the $\delta^{13}C$ of bulk leaf tissue of a coniferous forest and the specific leaf area
445 along an altitudinal gradient in the northern Rocky Mountains. Li MH et al. (2008) also
446 demonstrated that the specific leaf area of a dark coniferous forest decreased as the
447 altitude increased. However, there was a positive relationship between the $\delta^{13}C$ of bulk
448 leaf tissue and the specific leaf area for *Quercus aquifolioides* in a subalpine area of
449 western Sichuan Province (Li CY et al., 2009). There was also a negative relationship
450 between the $\delta^{13}C$ of bulk leaf tissue and the specific leaf area during the seasonal
451 variation of *Abies fabri* at 3000 m on Gongga Mountain (Luo TX et al., 2011). Nitrogen
452 is the main component of the photosynthetic enzyme and is also one of the main factors
453 that determine the photosynthetic capacity of a leaf. An increase in the leaf nitrogen
454 content can augment the content of leaf chlorophyll and carboxylase and therefore
455 influence the stomatal density and leaf thickness. Many studies have shown that the leaf
456 nitrogen content of alpine plants increases as the altitude increases (Friend et al., 1989;
457 Körner, 1989; Li CY et al., 2009). In the subalpine mountains, more nitrogen is
458 distributed to the leaf, thereby offsetting the decrease in photosynthetic rate caused by
459 low light and low nitrogen use efficiency.

460 Farquhar et al. (1982, 1989) showed that the stable carbon isotope composition of
461 leaf tissue was related to c_i/c_a. The stomatal conductance was influenced by climatic
462 variables and physiological function. In our study, both the value of c_i/c_a and c_i

Biogeosciences Discuss., doi:10.5194/bg-2015-652, 2016
Manuscript under review for journal Biogeosciences
Published: 11 February 2016
© Author(s) 2016. CC-BY 3.0 License.

463 decreased as the altitude increased. Therefore, both the transpiration and carbon gain
464 decreased along the altitudinal gradient (Fig. 6, 8). However, the way in which the
465 variation in the transpiration to carbon gain ratio responded to stomatal resistance under
466 changing environmental conditions was different. Keenan et al. (2013) also found that
467 the effects of stomatal control on the carbon gain and water loss were different. The
468 carbon gain is more sensitive to variations in conductance than the water loss (Li SE et
469 al., 2015). Therefore, GPP/T and NPP/T showed significant increases from low
470 altitudes to high altitudes, while the canopy interception increased along the elevation
471 gradient due to changes in the amount of rainfall. GPP/ET and NPP/ET only showed
472 moderately increasing trends along the elevation gradient.

473 **5 Conclusion**

474 Based on experimental data and modeled data, we analyzed the temporal and
475 altitudinal variations of the carbon gain, water loss and WUE and discussed the
476 mechanisms of climatic variables, specific leaf area and leaf nitrogen content that
477 control the carbon gain, water loss and WUE in a subalpine coniferous forest. WUE
478 was defined using different carbon gain and water loss components. On the monthly
479 scale, the carbon gain and water loss had different relationships with the precipitation,
480 air temperature, VPD and net radiation, indicating that a variety of climatic variables
481 drove the photosynthesis and ET in different ways and at different rates. On the
482 altitudinal scale, the carbon gain, ET and T decreased as the altitude increased, while
483 the GPP/T and NPP/T increased significantly as the altitude increased. However, the
484 GPP/ET and NPP/ET increased from 2800 to 3500 m and then decreased. Canopy

Biogeosciences Discuss., doi:10.5194/bg-2015-652, 2016
Manuscript under review for journal Biogeosciences
Published: 11 February 2016
© Author(s) 2016. CC-BY 3.0 License.

485 interception played an important role in the variation of WUE with different definitions
486 along the elevation gradient. WUE had a positive relationship with the specific leaf area
487 and a negative relationship with temperature and leaf nitrogen content along the
488 altitudinal gradient.

489 The response of the carbon gain and water loss to environmental and physiological
490 changes on the temporal and altitudinal scales is complex, which is also a great
491 challenge for water resource management and forest management. How the carbon gain,
492 water loss and WUE for the subalpine mountainous forest ecosystem varies with
493 changes in the global climate still remains to be investigated. Improved understanding
494 on temporal and altitudinal behavior of carbon and water vapour exchanges in relation
495 to environmental conditions will enhance our ability to predict the effects of changing
496 climate on mountainous ecosystems.

497 **Acknowledgements**

498 This study was supported by the Natural Science Foundation of China (No. 41401044
499 and No. 41310013) and the Chinese Academy of Science ('West Star' project).

500 **References**

501 Alice, M., Thomas, E., Eric, D., Caroline, L., Claire, D., 2011. Comparison of seasonal
502 variations in water use efficiency calculated from the carbon isotope composition
503 of tree rings and flux data in a temperate forest. Plant. Cell. Environ. 34,230-244
504 Beer, C., Ciais, P., Reichstein, M., Baldocchi, D., Law, B.E., Papale, D., Soussana, J.F.,
505 Ammann, C., Buchmann, N., Frank, D., Gianelle, D., Janssens, I.A., Knohi, A.,
506 Köstner, B., Moors, E., Roupsard, O., Verbeeck, H., Vesala, T., Williams, C.A.,

Biogeosciences Discuss., doi:10.5194/bg-2015-652, 2016
Manuscript under review for journal Biogeosciences
Published: 11 February 2016
© Author(s) 2016. CC-BY 3.0 License.

507 Wohlfahrt, G., 2009. Temporal and among-site variability of inherent water use
508 efficiency at the ecosystem level. Glob. Biogeochem. Cycles 23, GB2018
509 Bonal, D., Sabatier, D., Montpied, P., Tremeaux, D., Guehl, J.M., 2000. Interspecific
510 variability of ^{13}C among trees in rainforests of French Guiana: functional groups
511 and canopy interception. Oecologia 124,454-468
512 Cao, M., Woodward, F.I., 1998. Net primary and ecosystem production and carbon
513 stocks of terrestrial ecosystems and their responses to climate change. Glob.
514 Change. Biol. 4,185-198
515 Cochard, H., Martin, R., Gross, P., Bogeat-Triboulot, M.B. 2000. Temperature effects
516 on hydraulic conductance and water relations of Quercus robur L. J. Exp. Bot.
517 51,1255-1259
518 Deardorff, J.W., 1978. Efficient prediction of ground surface temperature and moisture,
519 with inclusion of a layer of vegetation. J. Geophys. Res. 83,1889-1903
520 Farquhar, G.D., von Caemmerer, S., Berry, J.A., 1980. A biochemical model of
521 photosynthetic CO_2 assimilation in leaves of C3 plants. Planta 149,78-90
522 Farquhar, G.D., Ehleringer, J.R., Hubick, K.T., 1989. Carbon isotope discrimination
523 and photosynthesis. Annu. Rev. Plant. Physiol. Plant. Mol. Biol. 40,503-537
524 Farquhar, G.D., O'Leary, M.H., Berry, J.A., 1982. On the relationship between carbon
525 isotope discrimination and the intercellular carbon dioxide concentration in leaves.
526 Aust. J. Plant. Physiol. 9,121-137
527 Friend, A.D., Woodward, F.I., Switsur, V.R., 1989. Field measurements of
528 photosynthesis, stomatal conductance, leaf nitrogen and $\delta^{13}C$ along altitudinal

Biogeosciences Discuss., doi:10.5194/bg-2015-652, 2016
Manuscript under review for journal Biogeosciences
Published: 11 February 2016
© Author(s) 2016. CC-BY 3.0 License.

529 gradients in Scotland. Funct. Ecol. 3,117-122

530 Gao, S.C., Wang, J.S., 2007. Analysis on current situation of forest resources in Tibet.
531 For. Resour. Manag. 5,49-52

532 Goulden, M.L., Anderson, R.G., Bales, R.C., Kelly, A.E., Meadows, M., Winstion,
533 G.C., 2012. Evapotranspiration along an elevation gradient in California's Sierra
534 Nevada. J. Geophys. Res. 117,G03028

535 He, Y.R., Liao, C.L., Zhang, B.H., 2005. A study on Pedography of soil on the Eastern
536 Slope of Mt. Gongga in Southeastern Qinghai-Tibet Plateau. J. Mt. Sci. 23,651-
537 656 (in Chinese with English abstract)

538 Huang, M., Ji, J.J., Li, K.R., Liu, Y.F., Yang, F.T. 2007. The ecosystem carbon
539 accumulation after conversion of grasslands to pine plantations in subtropical red
540 soil of South China. Tellus B 59,439-448

541 Hu, Z.M., Yu, G.R., Fan, J.W., Zhong, H.P., Wang, S.Q., Li, S.G., 2010. Precipitation-
542 use efficiency along a 4500-km grassland transect. Global. Ecol. Biogeogr.
543 19,842-851

544 Hultine, K.R., Marshall, J.D., 2000. Altitude trends in conifer leaf morphology and
545 stable carbon isotope composition. Oecologia 123,32-40

546 Huxman, T.E., Wilcox, B.P., Breshears, D.D., Scott, R.L., Snyder, K.A., Small, E.E., et
547 al., 2005. Ecohydrological implications of woody plant encroachment. Ecology
548 86,308-319

549 Ito, A., Inatomi, M., 2012. Water-use efficiency of the terrestrial biosphere: a model
550 analysis focusing on interactions between the global carbon and water cycles. J.

Biogeosciences Discuss., doi:10.5194/bg-2015-652, 2016
Manuscript under review for journal Biogeosciences
Published: 11 February 2016
© Author(s) 2016. CC-BY 3.0 License.

551 Hydrometeorol, 13,681-694

552 Ji, J.J., Hu, Y., 1989. A simple land surface process model for use in climate study. Acta.
553 Metetrol. Sin. 3,344-353

554 Ji, J.J., 1995. A climate-vegetation interaction model: simulating physical and
555 biological processes at the surface. J. Biogeogr. 22,2063-2069

556 Keenan, T.F., Hollinger, D.Y., Bohrer, G., Dragoni, D., Munger, J.W., Schimid, H.P.,
557 Richardson, A.D., 2013. Increase of forest water-use efficiency as atmospheric
558 carbon dioxide concentrations rise. Nature 499,324-327

559 Körner, C., 1989. The nutrient status of plants from high altitudes. Oecologia 81,379-
560 391

561 Lauteri, M., Pliura, A., Monteverdi, M.C., Brugnoli, E., Villani, F., Eriksson, G., 2004.
562 Genetic variation in carbon isotope discrimination in six European populations of
563 Castanea sativa Mill. Originating from contrasting localities. J. Evolution. Biol.
564 17,1286-1296

565 Law, B.E., Falge, E., Gu, L., Baldocchi, D.D., Bakwin, P., Berbigier, P., Davis, K.,
566 Dolman, A.J., Falk, M., Fuentes, J.D., Goldstein, A., Granier, A., Grelle, A.,
567 Hollinger, D., Janssens, I.A., Jarvis, P., Jensen, N.O., Katul, G., Mahli, K.,
568 Mattuecci, G., Meyers, T., Monson, R., Munger, W., Oechel, W., Olson, R.,
569 Pilegaard, K., Paw, U., Thorgeirsson, K.T., Valentini, H., Verma, R., Vesala, S.,
570 Wilson, T., Wofsy, K.S., 2002. Environmental controls over carbon dioxide and
571 water vapour exchange of terrestrial vegetation. Agric. For. Meteorol. 113, 97-120

572 Li, C.Y., Wu, C.C., Duan, B.L., Korpelainen, H., Luukkanen, O., 2009. Age-related

Biogeosciences Discuss., doi:10.5194/bg-2015-652, 2016
Manuscript under review for journal Biogeosciences
Published: 11 February 2016
© Author(s) 2016. CC-BY 3.0 License.

573 nutrient content and carbon isotope composition in the leaves and branches of
574 *Quercus aquifolioids* along an altitudinal gradient. Trees 23,1109-1121
575 Li, M.H., Xiao, W.F., Shi, P.L., Wang, S.G., Zhong, Y.D., Liu, X.L., Wang, X.D., Cai,
576 X.H., Shi, Z.M., 2008. Nitrogen and carbon source-sink relationships in trees at
577 the Himalayan treelines compared with lower elevations. Plant. Cell. Environ.
578 31,1377-1387
579 Li, S.E., Kang, S.Z., Zhang, L., Du, T.S., Tong, L., Ding, R.S., Guo, W.H., Zhao, P.,
580 Chen, X., Xiao, H., 2015. Ecosystem water use efficiency for a sparse vineyard in
581 arid northwest China. Agric. For. Meterol. 148,24-33
582 Li, J.Z., Wang, G.A., Liu, X.Z., Han, J.Y., Liu, M., Yang, X.J., 2009. Variations in
583 carbon isotope ratios of C3 plants and distribution of C4 plants along an altitudinal
584 transects on the eastern slope of Mount Gongga. Sci. China. Ser. D-Earth Sci.
585 39,1387-1396
586 Lin, Y., Wang, G.X., Guo, J.Y., Sun, X.Y., 2011. Quantifying evapotranspiration and its
587 components in a coniferous subalpine forest in Southwest China. Hydrol. Process
588 26,3032-3040
589 Lu, J.H., Ji, J.J., 2006. A simulation and mechanism analysis of long-term variations at
590 land surface over arid/semi-arid area in north China. J. Geophys. Res. 111,D09306
591 Luo, T.X., Luo, J., Pan, Y.D., 2005. Leaf traits and associated ecosystem characteristics
592 across subtropical and timberline forests in the Gongga Mountains, Eastern
593 Tibetan Plateau. Oecologia 142,261-273
594 Luo, T.X., Li, M.C., Luo, J., 2011. Seasonal variations in leaf $\delta^{13}C$ and nitrogen

Biogeosciences Discuss., doi:10.5194/bg-2015-652, 2016
Manuscript under review for journal Biogeosciences
Published: 11 February 2016
© Author(s) 2016. CC-BY 3.0 License.

595 associated with foliage turnover and carbon gain for a wet subalpine fir forest in
596 the Gongga Mountains, eastern Tibetan Plateau. Ecol. Res. 26,253-263
597 Lv, X.Y., Cheng, G.W., 2009. Climate change effects on soil carbon dynamics and
598 greenhouse gas emissions in Abies fabri forest of subalpine, southwest China. Soil.
599 Biol. Biochem. 41,1015-1021
600 Medlyn, B., De Kauwe, M. 2013. Biogeochemistry: carbon dioxide and water use in
601 forests. Nature 499,287-289
602 Monteith, J.L. 1965. Evaporation and environment, In: Fogg, G.E. (Ed.), The State and
603 Movement of Water in Living Organisms. Cambridge University Press,
604 Cambridge pp,205-234
605 Noilhan, J., Planton, S., 1989. A simple parameterization of land surface processes for
606 meteorological models. Mon. Weather. Rev. 117,536-549
607 Osmond, C.B., Winter, K., Ziegler, Z., 1982. Functional significance of different
608 pathways of CO2 fixation in photosynthesis. In *Encyclopedia of Plant Physiology,*
609 *New Series, Volume 128, Physiological Plant Ecology II, Water Relations and*
610 *Carbon Assimilation*. Springer-Verlag, Berlin pp,479-547
611 Panek, J.A., Warning, R.H. 1995. Carbon isotope variation in Douglas-fir foliage
612 improving the $\delta^{13}C$ –climate relationship. Tree. Physiol. 15,657-663
613 Parton, W.J., Schimel, D.S., Cole, C.V., et al., 1987. Division S-3-soil microbiology and
614 biochemistry: Analysis of factors controlling soil organic matter levels in great
615 plains grsslands. Soil. Sci. Soc. Am. J. 51,1173-1179
616 Parton, W.J., Scurlock, J.M.O., Ojima, D.S., et al., 1993. Observations and modelling

Biogeosciences Discuss., doi:10.5194/bg-2015-652, 2016
Manuscript under review for journal Biogeosciences
Published: 11 February 2016
© Author(s) 2016. CC-BY 3.0 License.

of biomass and soil organic matter dynamics for the grassland biome worldwide. Global. Biogeochem. Cycles. 7,785-809

Ponton, S., Flanagan, L.B., Alstad, K.P., Johnson, B.G., Morgenstern, K., Kljun, N., Black, T.A., Barr, A.G., 2006. Comparison of ecosystem water use efficiency among Douglas-fir forest, aspen forest and grassland using eddy covariance and carbon isotope techniques. Glob. Change. Biol. 12,294-310

Reichstein, M., Bahn, M., Mahecha, M.D., Kattge, J., Baldocchi, D.D., 2014. Linking plant and ecosystem functional biogeography. Proc. Natl. Acad. Sci. USA. 111,13697-13702

Saurer, M., Siegwolf, R.T.W., Schweingruber, F., 2004. Carbon isotope discrimination indicates improving water use efficiency of trees in northern Eurasia over the last 100 years. Glob. Change. Biol. 10,2109-2120

Shuttleworth, W.J., Wallace, J.S., 1985. Evaporation from sparse crop-an energy combination theory. Quart. J. R. Meteorol. Soc. 111,839-855

Steduto, P., Albrizio, R., 2005. Resource use efficiency of field-grown sunflower, sorghum, wheat and chickpea: II. Water use efficiency and comparison with radiation use efficiency. Agric. For. Meterol. 130,269-281

Sun, H.L., 2005. Ecosystems in China. Beijing Science Press (In Chinese)

Taylor, S.E., Sexton, O.J., 1972. Some implications of leaf tearing in Musaceae. Ecology 53,143-149

Van de Water, P.K., Leavitt, S.W., Betancourt, J.L., 2002. Leaf $\delta^{13}C$ variability with elevation, slope aspect and precipitation in the southwest United States. Oecologia

Biogeosciences Discuss., doi:10.5194/bg-2015-652, 2016
Manuscript under review for journal Biogeosciences
Published: 11 February 2016
© Author(s) 2016. CC-BY 3.0 License.

639 132,332-343

640 Vitousek, P.M., Field, C.B., Matson, P.A., 1990. Variation in foliar $\delta^{13}C$ in Hawaiian
641 Metrosideros polymorpha: a case of internal resistance? Oecologia 80,362-370

642 Wang, G.X., Deng, W., Yang, Y., Cheng, G.W., 2011. The Advances, Priority and
643 Developing Trend in Alpine Ecology. J. Mountain. Sci. 29,129-140 (In Chinese
644 with English abstract)

645 Wang, G.X., Ran, F., Chang, R.Y., Yang, Y., Luo, J., Fan, J.R., 2014. Variations in the
646 live biomass and carbon pools of Abies georgei along an elevation gradient on the
647 Tibetan Plateau, China. Forest. Eco. Manag. 329,255-263

648 Webb, E.K., Peaman, G.I., Leuning, R., 1980. Correction of flux measurement for
649 density effects due to heat and water vapor transfer. Quart. J. R. Meteorol. Soc.
650 106,85-100

651 Wilczak, J.M., Oncley, S.P., Stage, S.A., 2001. Sonic anemometer tilt correction
652 algorithms. Bound –Lay. Meteorol. 99(1),127-150

653 Wilson, K., Goldstein, A., Falge, E., Aubinet, M., Baldocchi, D., Berbigier, P.,
654 Bernhofer, C., Ceulemans, R., Dolmanh, H., Field, C., Grelle, A., Ibrom, W.,
655 Tenhunen, J., Valentini, R., Verma, S., 2002. Energy balance closure at FLUXNET
656 sites. Agric. For. Meterol. 113(1-4),223-243

657 Yu, G.R., Song, X., Wang, Q.F., Liu, Y.F., Guan, D.X., Yan, J.H., Sun, X.M., Zhang,
658 L.M., Wen, X.F., 2007. Water use efficiency of forest ecosystems in eastern China
659 and its relations to climatic variables. New. Phytol. 177,927-937

660

661

Biogeosciences Discuss., doi:10.5194/bg-2015-652, 2016
Manuscript under review for journal Biogeosciences
Published: 11 February 2016
© Author(s) 2016. CC-BY 3.0 License.

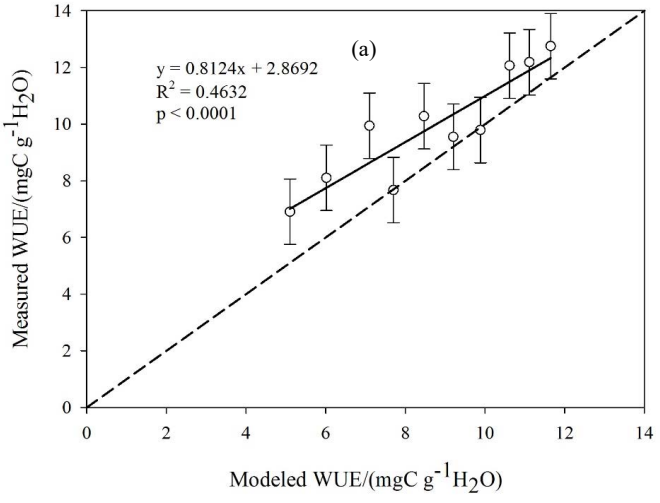

662

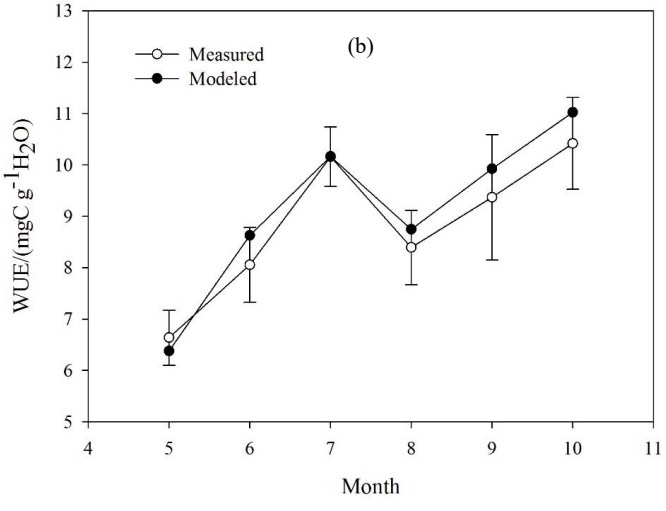

663

664 Fig. 1 Modeled and measured annual water use efficiency (WUE=GPP/Et) of *Abies*
665 *fabri* along an altitudinal gradient from 2800 m to 3700 m in 2011 (the dashed line is
666 1:1 line) (a), and temporal pattern from May to October on elevation of 3000 m in 2011
667 (b).

668

669

Biogeosciences Discuss., doi:10.5194/bg-2015-652, 2016
Manuscript under review for journal Biogeosciences
Published: 11 February 2016
© Author(s) 2016. CC-BY 3.0 License.

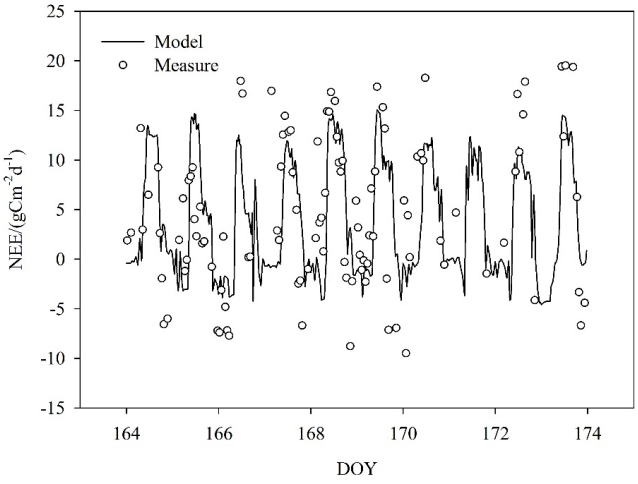

670

671 Fig. 2 Simulated NEE and the NEE deduced from eddy-covariance based
672 measurements over half an hour from the 164th to the 173rd day of 2009 at an altitude
673 of 3000 m (DOY is the day of year).

674

675

676

677

678

679

680

681

682

683

684

685

Biogeosciences Discuss., doi:10.5194/bg-2015-652, 2016
Manuscript under review for journal Biogeosciences
Published: 11 February 2016
© Author(s) 2016. CC-BY 3.0 License.

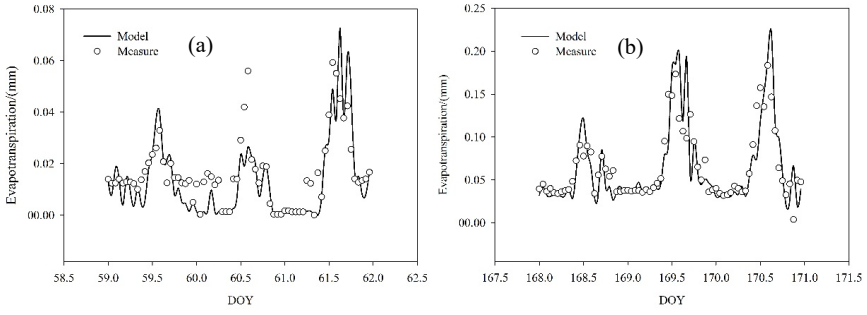

Fig. 3 Simulated ecosystem evapotranspiration (ET) and the ET deduced by eddy-covariance based measurements over half an hour from the 59th to the 61st (a) and the 168th to the 170th (b) days of 2009 at an altitude of 3000 m (DOY is the day of year).

Biogeosciences Discuss., doi:10.5194/bg-2015-652, 2016
Manuscript under review for journal Biogeosciences
Published: 11 February 2016
© Author(s) 2016. CC-BY 3.0 License.

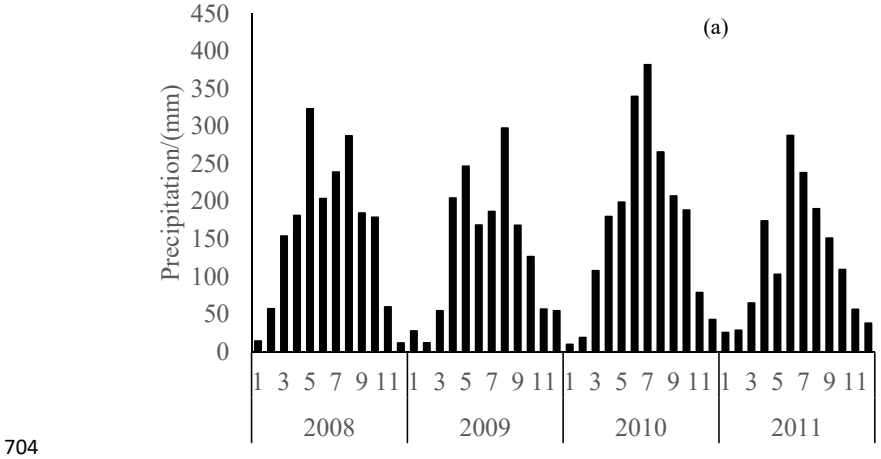

704

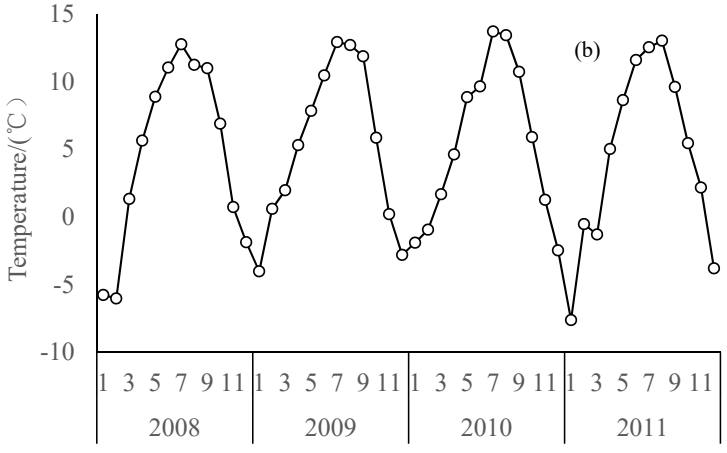

705

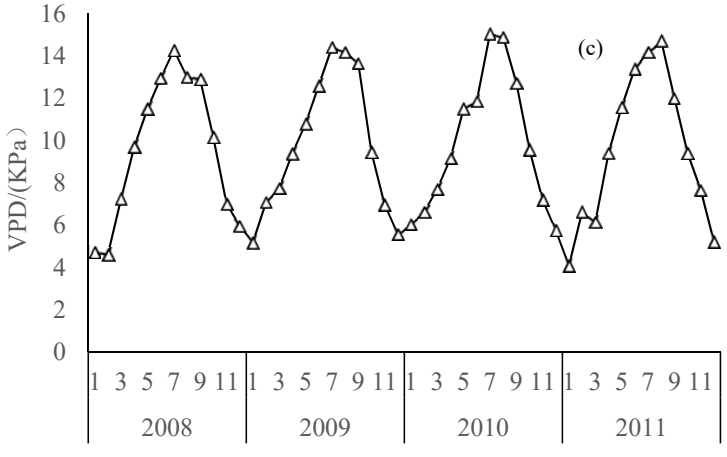

706

Biogeosciences Discuss., doi:10.5194/bg-2015-652, 2016
Manuscript under review for journal Biogeosciences
Published: 11 February 2016
© Author(s) 2016. CC-BY 3.0 License.

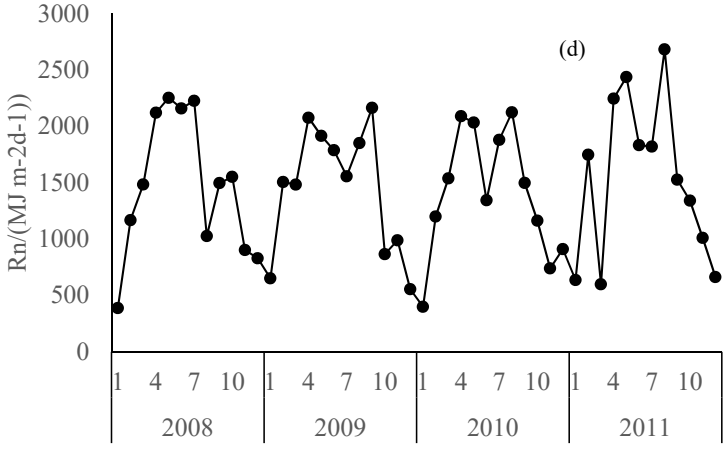

Fig. 4 The seasonal variation of precipitation (a), air temperature (b), VPD (c) and net radiation (d) from 2008 to 2011 at an altitude of 3000 m.

Biogeosciences Discuss., doi:10.5194/bg-2015-652, 2016
Manuscript under review for journal Biogeosciences
Published: 11 February 2016
© Author(s) 2016. CC-BY 3.0 License.

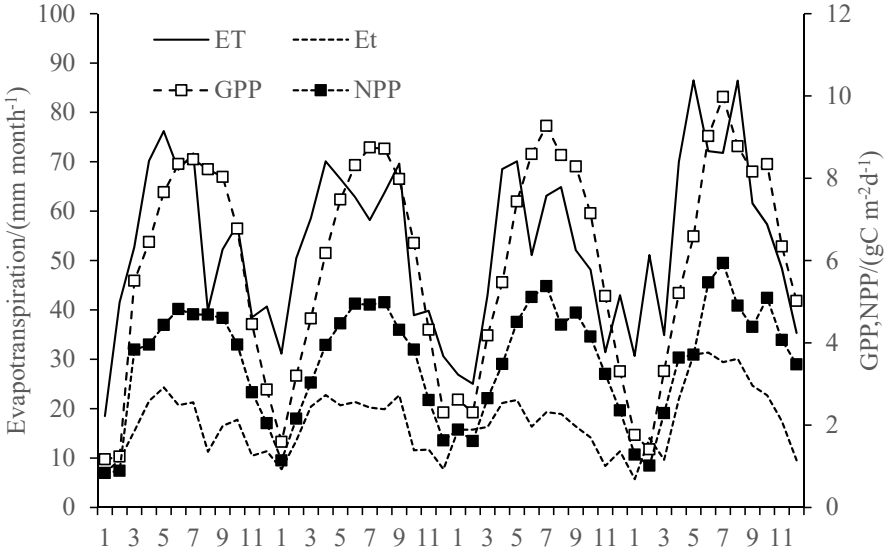

Fig. 5 The seasonal variation of monthly gross primary productivity (GPP), net primary productivity (NPP), evapotranspiration (ET) and transpiration (Et) simulated by the AVIM2 from 2008-2011.

Biogeosciences Discuss., doi:10.5194/bg-2015-652, 2016
Manuscript under review for journal Biogeosciences
Published: 11 February 2016
© Author(s) 2016. CC-BY 3.0 License.

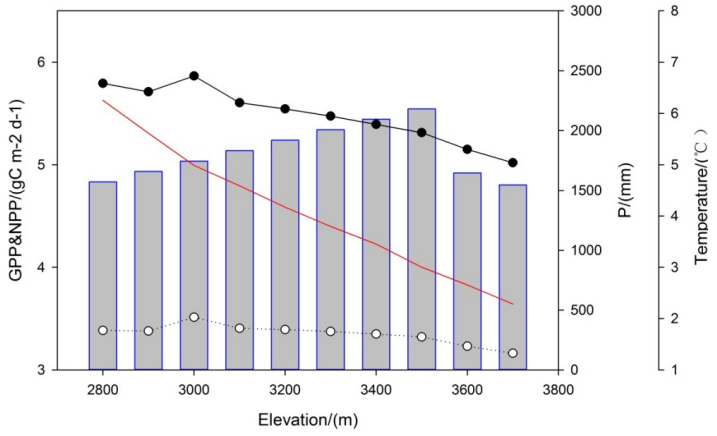

730

731 Fig. 6 Precipitation, temperature, GPP and NPP change along an altitudinal gradient
732 from 2800 to 3700 m on Mt. Gongga (the solid line with solid circles is GPP, the
733 dashed line with hollow circles is NPP, the red line is air temperature, and the gray
734 bar is precipitation).

735

736

737

738

739

740

741

742

743

744

745

Biogeosciences Discuss., doi:10.5194/bg-2015-652, 2016
Manuscript under review for journal Biogeosciences
Published: 11 February 2016
© Author(s) 2016. CC-BY 3.0 License.

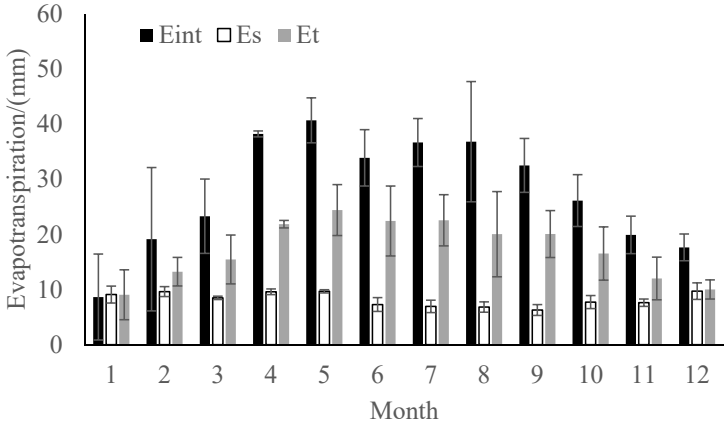

Fig. 7 Seasonal variation in the components of evapotranspiration (mean ± SE) at an altitude of 3000 m in 2012 (Eint is canopy interception, Es is soil evaporation, Et is transpiration). Eint, Es and Et were simulated by the AVIM2.

Biogeosciences Discuss., doi:10.5194/bg-2015-652, 2016
Manuscript under review for journal Biogeosciences
Published: 11 February 2016
© Author(s) 2016. CC-BY 3.0 License.

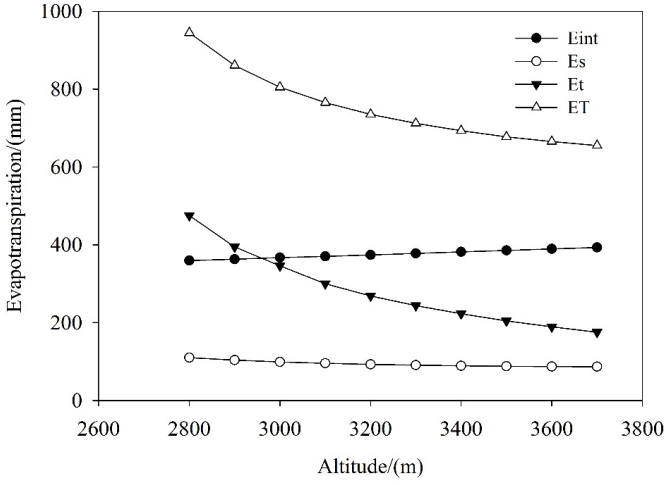

762

763 Fig. 8 Variation in evapotranspiration (ET) and its components (canopy interception,

764 Eint; soil evaporation, Es; transpiration, Et) along an altitudinal gradient between

765 2800 and 3700 m.

766

767

768

769

770

771

772

773

774

775

776

Biogeosciences Discuss., doi:10.5194/bg-2015-652, 2016
Manuscript under review for journal Biogeosciences
Published: 11 February 2016
© Author(s) 2016. CC-BY 3.0 License.

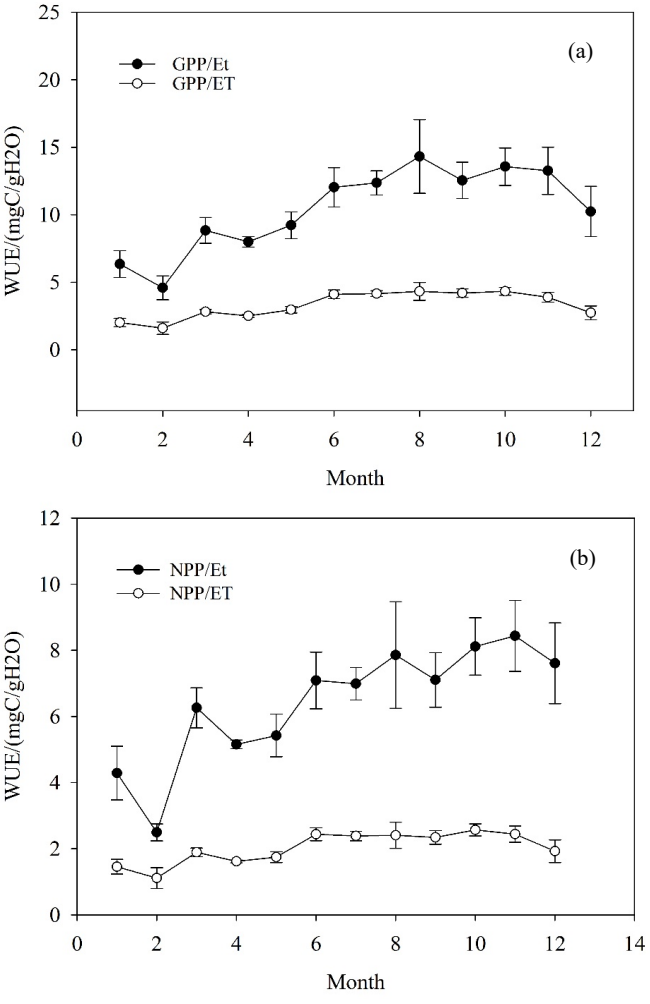

Fig. 9 The simulated seasonal variation of GPP/Et (mean ± SE), GPP/Etotal (mean ± SE), NPP/Et (mean ± SE) and NPP/Etotal (mean ± SE) on Mt. Gongga.

Biogeosciences Discuss., doi:10.5194/bg-2015-652, 2016
Manuscript under review for journal Biogeosciences
Published: 11 February 2016
© Author(s) 2016. CC-BY 3.0 License.

783

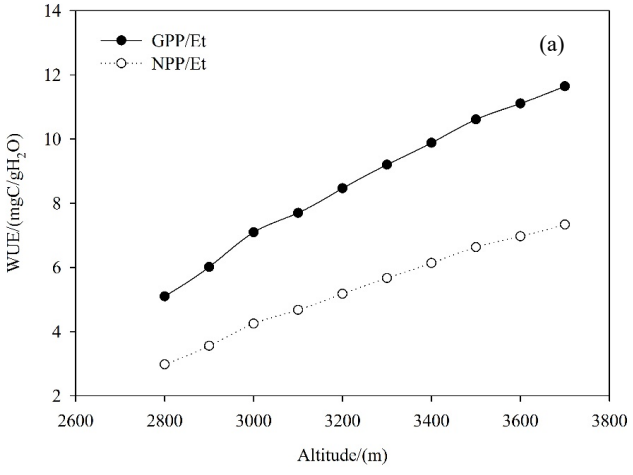

784

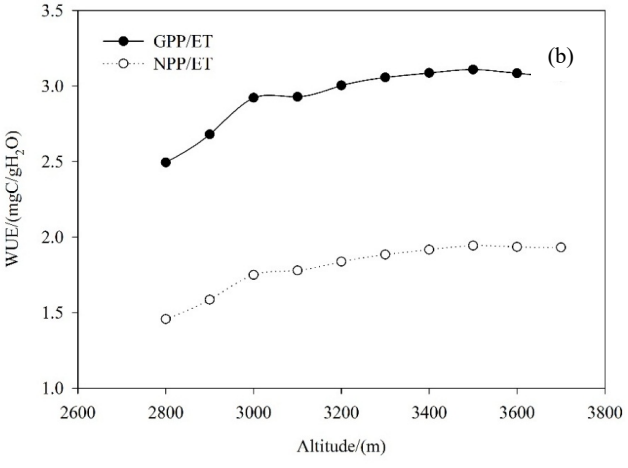

785 Fig. 10 The simulated spatial variation of GPP/Et, GPP/ET, NPP/Et and NPP/ET

786 along an altitudinal gradient from 2800 to 3700 m on Mt. Gongga.

Biogeosciences Discuss., doi:10.5194/bg-2015-652, 2016
Manuscript under review for journal Biogeosciences
Published: 11 February 2016
© Author(s) 2016. CC-BY 3.0 License.

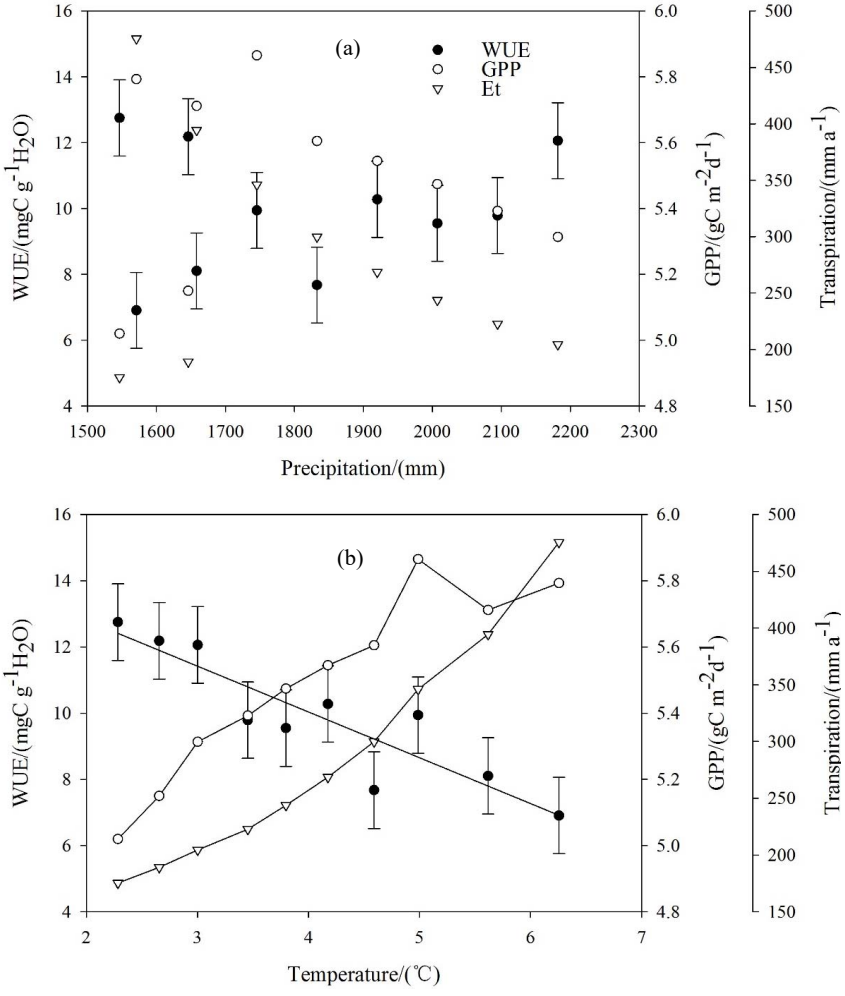

Fig. 11 The relationship between water use efficiency (derived from $\delta^{13}C$ of bulk leaf tissue) (black solid circles with standard error), GPP (black open circles), Et (black open triangles) and precipitation (a) or temperature (b) along an altitudinal gradient from 2800 m to 3700 m.

Biogeosciences Discuss., doi:10.5194/bg-2015-652, 2016
Manuscript under review for journal Biogeosciences
Published: 11 February 2016
© Author(s) 2016. CC-BY 3.0 License.

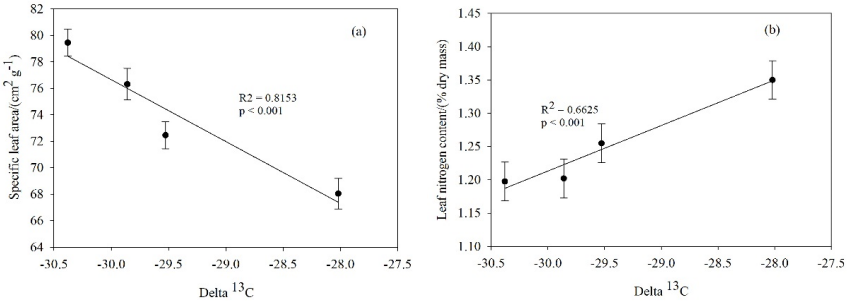

796

797 Fig. 12 The relationship between the $\delta^{13}C$ of bulk leaf tissue and the specific leaf area

798 or the leaf nitrogen content along an altitudinal gradient from 2800 m to 3700 m.

799

800

801

802

803

804

805

806

807

808

809

810

811

812

Biogeosciences Discuss., doi:10.5194/bg-2015-652, 2016
Manuscript under review for journal Biogeosciences
Published: 11 February 2016
© Author(s) 2016. CC-BY 3.0 License.

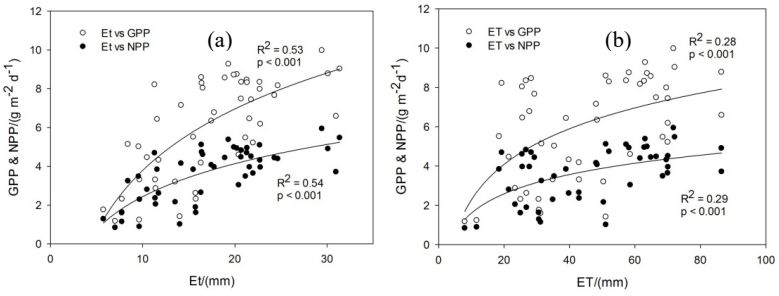

Fig. 13 The relationship between monthly gross primary productivity (GPP), net primary productivity (NPP), transpiration (Et) and evapotranspiration (ET) at an altitude of 3000 m from 2008 to 2011 ($y = a \bullet \ln x + b$).

Biogeosciences Discuss., doi:10.5194/bg-2015-652, 2016
Manuscript under review for journal Biogeosciences
Published: 11 February 2016
© Author(s) 2016. CC-BY 3.0 License.

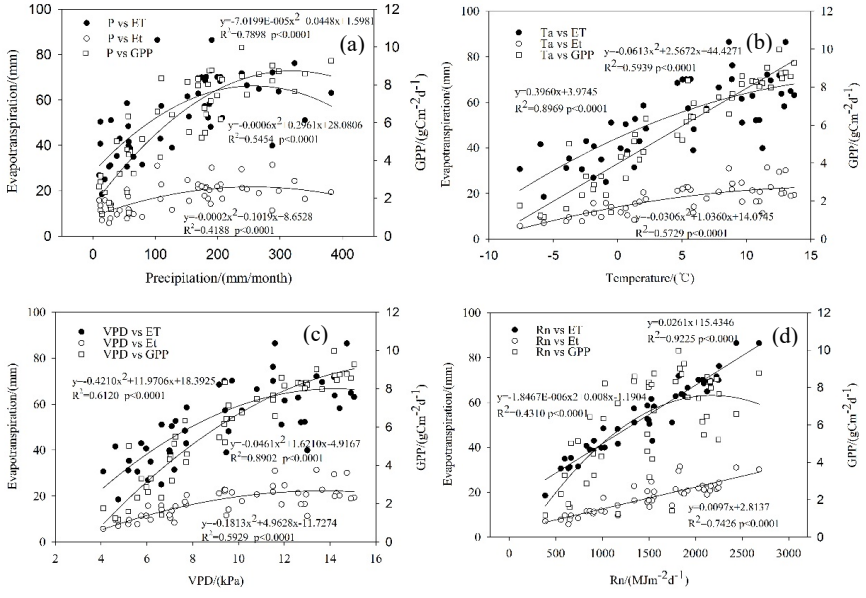

Fig. 14 The relationship between monthly evapotranspiration (ET), transpiration (Et), gross primary productivity (GPP), and climatic variables (precipitation, temperature, saturated vapor pressure deficit (VPD) and net radiation (R_n)) at an altitude of 3000 m from 2008 to 2011.

Biogeosciences Discuss., doi:10.5194/bg-2015-652, 2016
Manuscript under review for journal Biogeosciences
Published: 11 February 2016
© Author(s) 2016. CC-BY 3.0 License.

847 Table 1 Variation in precipitation every 100 m along an altitudinal gradient using

848 four meteorological stations at each site

	2800-3000	3000-3500	3500-3700
Precipitation variation	+5%/100 m	+5%/100 m	-5.7%/100 m

849